Research on scan polishing flat surfaces with a small diameter tool

He Wang[1, a], Weimin Lin[1, b *]

[1]Division of Mechanical Science and Technology, Graduate School of Science and Technology, Gunma University, 1-5-1 Tenjin-cho, Kiryu-shi, Gunma Prefecture 376-8515, Japan

[a]email:wanghebape@126.com, [b]email:w-lin@palette.plala.or.jp

Keywords: NiP, Finishing, Material removal velocity, Polishing models

Abstract. High profile accuracy and high surface quality, which are achieved by stable polishing velocity, are needed in the machining of NiP neutron reflection mirror along with suitable machining tools. To respond to the growing demands for high quality reflection mirrors, in this study, a small diameter polishing tool was used on a three-axis CNC ultra-precise polishing machine. Mathematical models of polished profiles based on the Preston equation were built and discussed along with the simulation results of the polished profiles. These models of polished profiles were proved to be effective by numerous experiments under diverse conditions. The polishing characteristics of electro-less plated NiP surface were reviewed and super smooth surfaces could be achieved by scan-type polishing.

Introduction

The optical control of the neutron beam is an innovative research area as it is used in organic structure determination and medical treatment more widely than X-ray. On the other hand, the excellent machinability by polishing of electro-less plated NiP makes it one of the best materials for making neutron reflection mirrors.

Unlike X-ray, which is used widely for the superficial analysis of materials, neutron beam shows greater ability to recognize the probe structure of material atoms and molecules. However, owing to the difficulty of direction control, operation complexity, and low cost-effectiveness, the areas of application of neutron are limited [1]-[3]. The electron-less plated NiP has been demonstrated to be an ideal candidate for the neutron reflection mirror as it does not have any of the drawbacks of neutron beam [4]-[7].

High profile accuracy and high surface quality, which are achieved by stable polishing velocity, are needed in the machining of NiP neutron reflection mirror along with suitable machining tools [8]-[10]. To respond to the growing demands for high quality reflection mirrors, in this study, a small-diameter polishing tool was used on a three-axis CNC ultra-precise polishing machine. This method is capable of stable polishing velocity, thereby realizing stable polished work surface. When the tool moves along the complex polishing paths, the polishing directions are changed frequently, and the polishing stabilities are reduced. The conventional polishing material removal models can only predict the removal depth at the fixed grinding points.

In this work, we applied an empirical formula of the removal profile based on the Preston equation, and proved by experiments that we can control polishing shapes. The fundamental polishing characteristics of scan-type polishing are also discussed in this paper. Free-form surfaces could be processed by using different parameters in computer numerical control (CNC) [11,12].

Experimental Procedure

Figure 1 shows the three-axis CNC ultra-precise polishing machine which consists of the body and controller. Figure 2 shows a schematic of the three-axis CNC ultra-precise polishing control system. The movements of the XYZ axes are controlled by the PC while the rotation speeds are controlled by the motor controller.

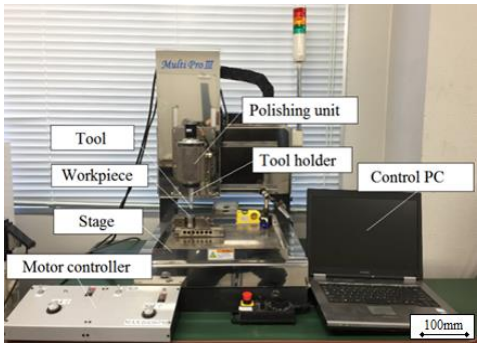

Fig. 1 Photograph of experimental system

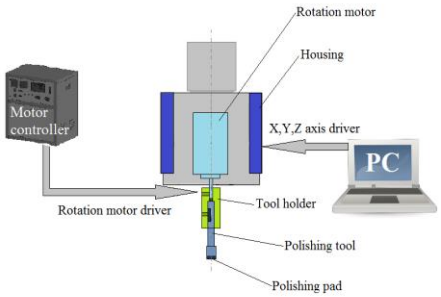

Fig.2 Schematic of three-axis polishing control system

All experiments were carried out by a 3-axis simultaneous control desk-top polishing device with a resolution of 0.001 mm. Figure 3 shows a photograph of the experimental setup. During the polishing process, abrasive was dripped on the polishing zone through an abrasive nozzle. The workpiece was made of electro-less plated NiP. The polishing tool (ϕ5 mm) was used in scan-type polishing in Figure 4.

Fig. 3 Photograph of experimental setup

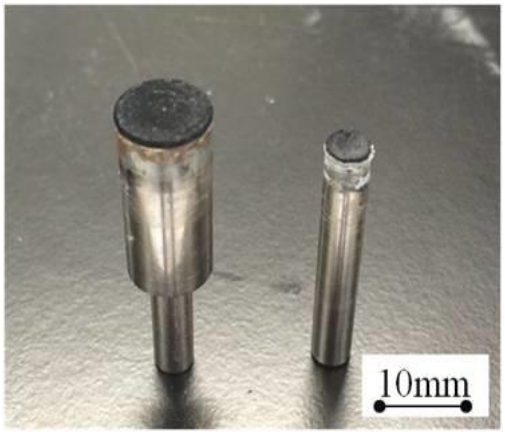

Fig.4 Photograph of scan polishing tool (left: ϕ10 mm, right: ϕ 5 mm)

Figure 5 shows XY and YX scan paths used in the polishing experiments. In actual XY-YX polishing process, the XY scan path is applied first, followed by the YX scan. Scan pitch was discussed by numerous experiments under diverse conditions. Subsequently, we polished the whole square plane of the workpiece surface by the XY and XY-YX type method. The polishing characteristics of electro-less plated NiP surface were reviewed and super smooth surfaces could be achieved by scan-type polishing. The single path polishing method was carried out in the last part to prove that the proposed mathematical model was effective.

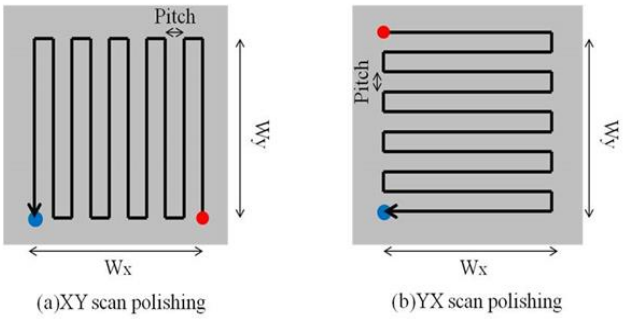

Fig. 5 Polishing scan path

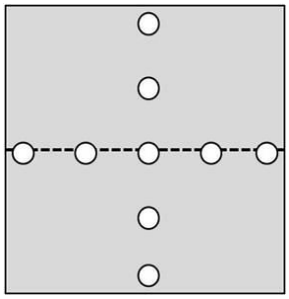

Fig.6 Measurement point of scan polishing

A general sense of surface smoothness can be seen and then research surface roughness using a measuring device 3D Optical Surface Profilers (NewView600, ZygoCo., Ltd.). As shown in Figure 6, the surface roughness of the workpiece (50mm×50mm) was measured at 9 white area and taken the average. To review the polishing characteristics and prove the proposed mathematical model of electro-less plated NiP surface, we performed free abrasive polishing on the Electro-less plated NiP under these conditions as shown in Table 1.

Table 1 Main experimental conditions

Experimental conditions	Values
Workpiece material	Electro-less plated NiP surface
Tool diameter	5mm
Tool rotational speed	300 rpm
Tool moving speed	240mm/min
Abrasive material	Colloidal silica abrasive 10 wt %(23nm)
Polishing pressure	25kPa
Abrasive supply	0.05 g
Scan method	XY scan, XY-YX scan, Single path
Scan pitch	0.5mm

Experimental results and discussion

Figure 7 shows the relationship between sojourn time and surface roughness of each scan pitch in XY scan. After polishing about 13 minutes to generate smooth surface (Ra 5 nm) through comparing pitch 0.5 mm and pitch 0.05 mm. Figure 8 shows the photograph of surface condition after polishing about 5 minutes with scan pitch 0.5 mm and 2.5 mm in XY scan.

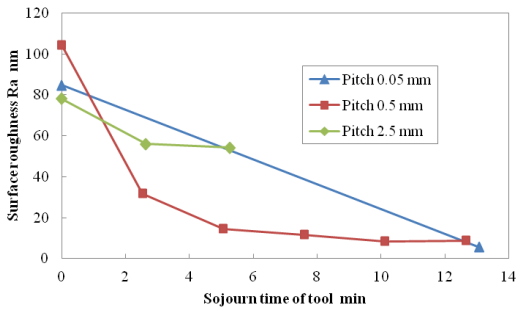

Fig. 7 Relationship between sojourn time and surface roughness with different scan pitch

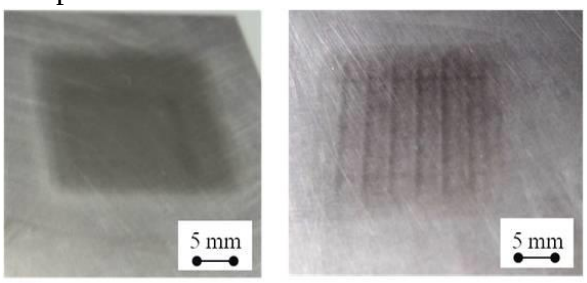

(a)Pitch 0.5 mm (b)Pitch 2.5 mm

Fig. 8 Photograph of surface condition with scan pitch 0.5 mm and 2.5 mm

The surface was uniformly polished at a pitch of 0.5 mm, whereas at a pitch of 2.5 mm, traces of the polishing tool passed through the surface could be seen. When the pitch is large, the fluctuation of surface and the period become larger. When the pitch is relatively small, the fluctuation of surface and the period become smaller. And polishing unevenness occurred at a relatively large pitch 2.5 mm. In the three scan pitches used in this experiment, the material removal is relatively small, and the smoother surface is generated with pitch 0.5mm. This pitch 0.5 mm is used in the following experiments.

Figure 9 shows the comparison between cross-section shape of XY and XY-YX scan polishing. From the measured data, the profile of cross-section was calculated, and material removal of the polished area and polishing depth were obtained. Compared with XY scan polishing, smoother and material removal can be achieved by using XY-YX scan polishing method.

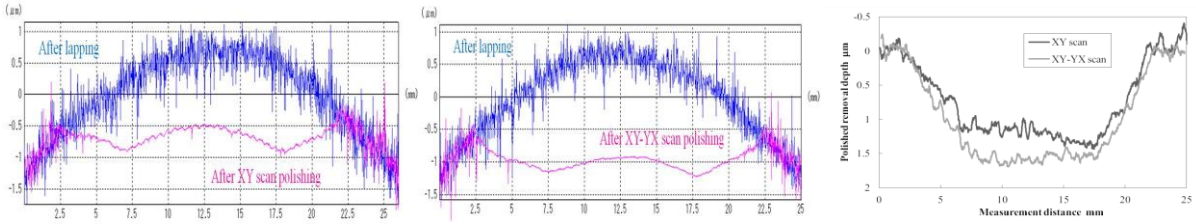

(a) XY scans polishing (b) XY-YX scans polishing (c) Removal depth of XY scan and XY-YX scan polishing

Fig.9 Comparison between cross-section shape of scan polishing

Figure 10 (a) shows the relationship between the polishing time and surface roughness in the XY scan and XY-YX scan polishing. The same trend can be seen where the roughness decreases during the XY scan polishing and XY-YX scan polishing after 12 minutes of polishing. It was found that surface roughness of both path was improved to Ra 1.7 nm after 30 minutes. There is little to differentiate between the surface roughness of the two polishing paths. Figure 10 (b) shows enlarged view of cross-section shape. The scan pitch of the surface is non-smooth in the XY scan polishing. Smoother surface was formed by XY-YX scan polishing path with flat surface and without distortion.

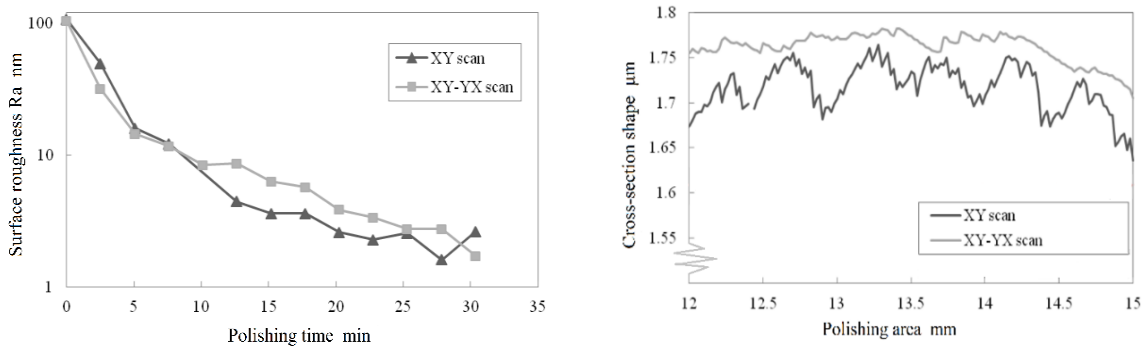

(a)surface roughness (b) enlarged view of cross-section shape

Fig. 10 Relationship between polishing time and surface roughness with XY scan and XY-YX scan polishing

Figure 11 shows photographs of the workpiece with different surface roughness before and after 15 minutes of XY-YX scan polishing. After polishing to generate mirror surface (Ra 0.12 nm), the reflection of the text could be seen.

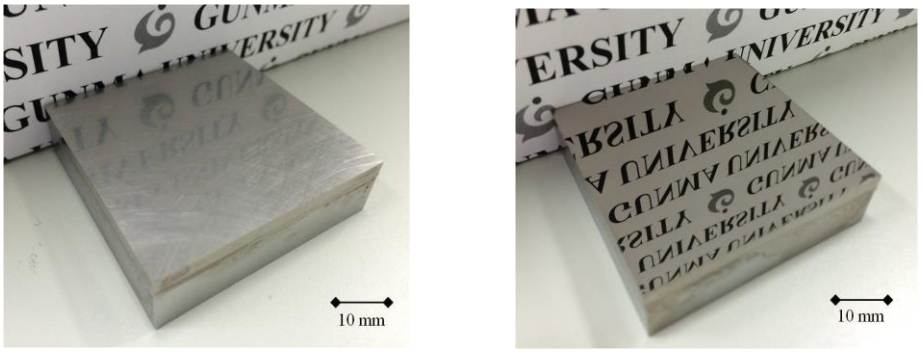

(a)before polishing (b)processed surface

Fig. 11 Photograph of electro-less plated NiP

Model formulation and validation

The function of material removal is expressed by Eq.(1) based on the Preston equation, where k is the Preston wear coefficient (measured by experiments), t is the polishing time, P and V are pressure and relative velocity distribution function in the polishing area, respectively [13]-[16].

$$\delta = k \cdot P \cdot V \cdot t \tag{1}$$

A new mathematical model was designed for calculating the sizes and shapes of removal areas. A Cartesian coordinate system was introduced for clarity, and the z-axis direction was defined as the opposite of the material removal depth (Figure 12). When the tool moves at a certain feed velocity v_f, the coordinate system o-xy is established at the central point O, which sits on the polishing path[17]-[20]. In the tangent plane of point P, x and y are defined as the vertical and tangential directions of the path, respectively.

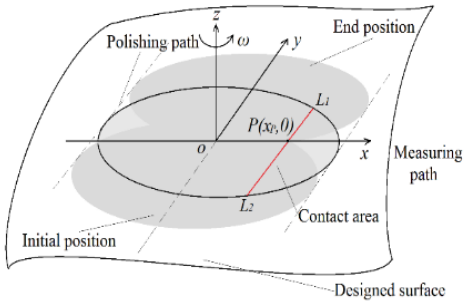

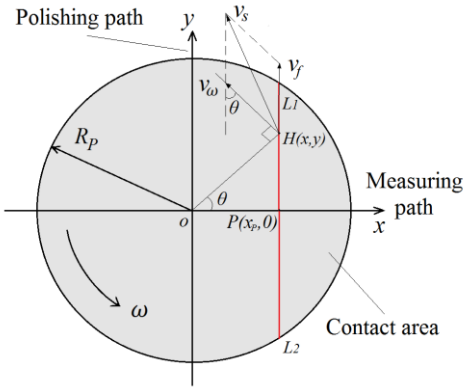

Fig.12 Definition of polishing area coordinate systems **Fig. 13** Polishing area velocity distribution

In the coordinate system (Figure 12), point P is located in the x-direction in the contact area, p_c refers to the pressure of point P, and v_s is the relative speed between the tool and workpiece. Based on Preston principle, it is possible to determine the removal depth during time dT using Eq.(2).

$$dh = k_p p_c v_s dT \tag{2}$$

The path length of the tool during that time is,

$$dl = dT v_f \quad (3)$$

By substituting Eq.(2) with Eq.(3), the material removal depth of per unit path length (E) can be obtained by Eq.(4)

$$E = \frac{dh}{dl} = k_p \frac{p_c v_s}{v_f} \quad (4)$$

The removal depth of point P is the summation composed of each infinitesimal element on the line L1L2. The material removal depth per unit path length, which acts as an infinitesimal element, is related to the pressure and relative velocity of various points in polishing areas. The removal depth of the polished area can be obtained by Eq.(5)

$$h = \int_{L_2}^{L_1} E \, dl \quad (5)$$

The distribution of pressure is homogeneous in the contact area. Eq.(6) shows the pressure distribution function of the polishing area, where F_n is the normal force of the polishing tool.

$$p_c = \frac{F_n}{\pi R_p^2} \quad (6)$$

The relative velocity of various points of the polishing area is not uniform, and their distribution functions are related to the angles of rotation and processing pose as well [21,22]. Figure 13 shows the velocity distribution in the contact area, where w is the rotation angular velocity of the tool, v_ω is the linear velocity of any point H in the polishing area, while θ is the angle between the direction of the linear velocity of point H and the polishing path. According to the motional regularity and geometric relation, the linear velocity of point H can be expressed by Eq.(7).

$$v_\omega = \omega\sqrt{x^2 + y^2} \quad (7)$$

$$\cos\theta = \frac{x}{\sqrt{x^2+y^2}} \quad (8)$$

Therefore, based on the velocity composition law of particle movement, the relative speed v_s between the tool and workpiece surfaces can be obtained by Eq.(9).

$$v_s = \sqrt{v_f^2 + v_\omega^2 + 2v_f v_\omega \cos\theta} \quad (9)$$

The removal depth and shape of the polished area can be simulated by Eq.(10) , where the Preston wear coefficient k_P can be obtained through experiments. The depth of point P is the summation of each infinitesimal element in the polishing area.

$$h(x) = \frac{2k_P F_n}{v_f \pi R_P^2} \int_0^{\sqrt{R_P^2 - x^2}} v_s \, dy \quad (10)$$

To calculate the Preston coefficient k_P , the following parameters were needed: the mass difference of workpiece after polishing, relative speed v_s, polishing force F_n, and density of the workpiece ρ_d. After several experiments and linear fitting calculation of the experimental data, we successfully obtained a more accurate k_P value. Polishing experiments were carried out for the specified single path using a small diameter tool, and the polishing profiles of the removal functions (polished amount, surface roughness, etc.) are compared and discussed below.

The red curves indicate the simulation results of the theoretical removal profiles of a single path using the Matlab software, and the blue curves, measured using a non-contact surface profile measuring device (Mitaka Kohki Co., Ltd. PF-60), indicates the experimental section profile of a single path (Figure 14). From the measured data, the cross-section of the

hemispheric polished area center profile was calculated, and the diameters of the polished area and polishing depth were obtained. The experimental and theoretical polished profiles of the single path show agreement in Figure 14, which validates the model proposed in this study. Given the thin disc-shaped polishing pad, the shape of the end remains essentially unchanged as the polishing tool kept with stable polishing velocity along the process. The polishing tool wear can be ignored.

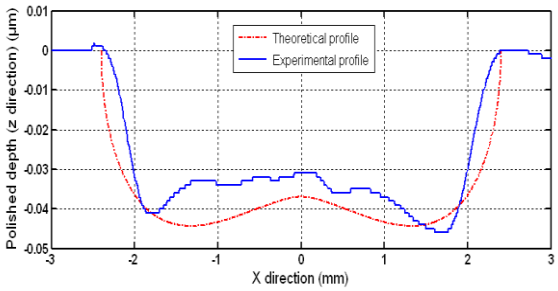

Fig. 14 Difference between theoretical and experimental profiles of single path

Conclusion and outlook

A new removal model based on the Preston principle which combines material characteristics and integral calculus was proposed and discussed. The characteristics of the surface roughness were also illustrated.

The algebraic expression of the removal profile was derived from the infinitesimal polishing depth at each dwell point of the polishing process.

Using our model, the removal profile could be calculated by the processing conditions, material mechanics and physical properties, and geometry relations of workpieces and tools. The results showed that the proposed mathematical model can be applied for planning the deterministic polishing process by the precise simulation of the material removal depth of the work surface.

Moreover, this XY-YX scan path can polish workpieces with high surface quality in the limited dimension of the machine tool. Ra 0.12 nm surface roughness can be achieved 15 minutes after the start of polishing.

Acknowledgement

This work was supported by JSPS KAKENHI Grant Numbers JP22360062, JP22560125. We would like to thank Ms. Haruko Mashimo of Gunma University for supporting this experiment.

References

[1] M. Furusaka et al.: “First results from a mini-focusing small-angle neutron scattering instrument (mfSANS) with an ellipsoidal mirror”, ICANS-XVIII, Dongguan, China, April 25-29 (2007) D3-2.

[2] K. Hirota et al., Development of a neutron detector based on a position-sensitive photomultiplier, Phys. Chem. Chem. Phys. 7 1836-1838(2005).

[3] W Lin, H Ohmori, Y Yamagata, S Moriyasu, T Kasai, K Horio, C Liu. A Polishing Method of Large X-Ray Mirror Surface. Advances in Abrasive Technology 2000; 3:175.

[4] H. Yasui et al.: High Removal Rate Ultra-Smoothness Polishing of NiP Plated Aluminum Magnetic Disk Substrate by Means High Polishing Speed with High Polishing Pressure, Proc. ASPE 2002 Annual Meeting, Vol.27 (2002) p. 689-692.

[5] Kinast, J., Hilpert, E., Lange, N., Gebhardt, A., Rohloff, R.-R., Risse, S., Eberhardt, R., and Tünnermann, A.,"Minimizing the bimetallic bending for cryogenic metal optics based on electroless nickel," Proc. SPIE 9151,915136-1-915136-9 (2014).

[6] Gebhardt, A., Kinast, J., Rohloff, R.-R., Seifert, W., Beier, M., Scheiding, S., and Peschel, T., "Athermal Metal Optics made of Nickel plated AlSi40," Proc. ICSO 2014, 1-8 (2014).

[7] Kinast, J., Grabowski, K., Gebhardt, A., Rohloff, R.-R., Risse, S., and Tünnermann, A., "Dimensional Stability of Metal Optics on Nickel plated AlSi40," Proc. ICSO 2014, 1-8 (2014).

[8] Steinkopf, R., Gebhardt, A., Scheiding, S., Rohde, M., Stenzel, O., Gliech, S., Giggel, V., Löscher, H., Ullrich, G.,Rucks, P., Duparre, A., Risse, S., Eberhardt, R., and Tünnermann A., "Metal mirrors with excellent figure and roughness," SPIE 7102, 71020C-1-71020C-12 (2008).

[9] W Lin, T Kasai, K Horio, T Doi. Surface Characteristics of the Polyurethane Polisher in Mirror-Polishing Process. Precis Eng 1999;65:1147

[10] T Tanakak. Manufacturing method of non-aspheric lens and super-precision non-aspheric surface machine. Optical Technology Contact 2000;38(10):592-599.

[11] RA Jones. Computer controlled optical surfacing with orbital tool motion. Opt Eng 1986; 25(6): 785–790.

[12] Jones RA. Optimization of computer controlled polishing. Appl Opt 1977;16(1):219–224.

[13] G Savio, R Meneghello, G Concheri. A surface roughness predictive model in deterministic polishing of ground glass moulds. Int J Mach Tool Manu 2009;1–7.

[14] FW Preston. The theory and design of glass plate polishing machines. J Soc Glass Technol 1927;11: 247–256.

[15] DW Kim, SW Kim. Static tool influence function for fabrication simulation of hexagonal mirror segments for extremely large telescopes. Opt Express 2005;910–917.

[16] C Fan. Predictive models of the local and the global polished profiles in deterministic polishing of free-from surfaces. Journal of Engineering Manufacture 2014; 228(8):868-879

[17] JF Song, XY Yao, DG Xie, et al. Effects of polishing parameters on material removal for curved optical glasses in bonnet polishing. Chin J Mech Eng 2008;29–33.

[18] MY Yang, HC Lee. Local material removal mechanism considering curvature effect in the polishing process of the small aspherical lens die. J Mater Process Tech 2001;116(2):298–304.

[19] JS Lee, K Soyji. A study on ultra precision machining for aspherical surface of optical parts. Journal of the Korean Society of Precision Engineering 2002;19(10):195-201.

[20] Klocke F, Dambon O, Zunke R. Modeling of contact behavior between polishing pad and workpiece surface. Prod Eng 2008;9-14.

[21] TI Suratwala, MD Feit, WA Steele. Toward deterministic material removal and surface figure during fused silica pad polishing. J Am Ceram Soc 2010;1326-1340.

[22] SD Jacobs, D Golini, Y Hsu, BE Puchebner, D Strafford, WI Lordonski, IV Prokhorov, E Fress, D Pietrowski, VW Kordonski.Magneto-rheological finishing: A deterministic process for optics manufacturing. SPIE 1995; 372:2576.